

CHAPTER TWO

DISLOCATION THEORY STRENGTHENING OF MATERIALS



Dislocation Theory and strengthening of Materials

Dislocations and Strengthening Mechanisms

What is happening in material during plastic deformation?

▪ Dislocations and Plastic Deformation

- ✓ Motion of dislocations in response to stress
- ✓ Slip Systems
- ✓ Plastic deformation in
 - single crystals
 - polycrystalline materials

▪ Strengthening mechanisms

- ✓ Grain Size Reduction
- ✓ Solid Solution Strengthening
- ✓ Strain Hardening

▪ Recovery, Recrystallization, and Grain Growth

Not tested: 7.7 Deformation by twinning,

Direction and plane nomenclature in §7.4.

Introduction

theory of dislocation behavior was developed extensively and applied to practically every aspect of the plastic deformation of metals. Because there were no really reliable methods for detecting dislocations in real materials, it was necessary to build much of this theory on the basis of indirect observations of dislocation behavior. However, in the last 20 years extensive research has developed a variety of techniques for observing and studying dislocations in real materials. These studies leave no doubt that dislocations exist, and more importantly, they have provided experimental verification for most of the theoretical concepts of dislocation theory.

Practically all the experimental techniques for detecting dislocations utilize the strain field around a dislocation to increase its effective size. These experimental techniques can be roughly classified into two categories, those involving chemical reactions with the dislocation, and those utilizing the physical changes at the site of a dislocation.¹ Chemical methods include etch-pit techniques and precipitation techniques. Methods based on the physical structure at a dislocation site include transmission electron microscopy of thin films and x-ray diffraction techniques.

The simplest chemical technique is the use of an etchant which forms a pit at the point where a dislocation intersects the surface. Etch pits are formed at dislocation sites because the strain field surrounding the dislocation causes preferential chemical attack. A great deal of information about dislocation behavior in the ionic crystal LiF has been obtained in this way by Gilman and Johnston.² Important information about dislocations in metals has also been obtained with etch-pit techniques. Figure 5-1 shows the excellent resolution obtainable from etch-pit studies on alpha brass.³ Pits only 500 Å (= 50 nm) apart have been resolved. In the region of heavy slip shown in this electron micrograph the dislocation density is 10^{10} cm^{-2} (= 10^8 mm^{-2}).

In metals, etch-pit formation at dislocations appears to be dependent on purity.⁴ Because of solute segregation to the dislocation, the region around the dislocation becomes anodic to the surrounding metal, and consequently preferential etching occurs at the dislocation. Figure 6-4 shows an etch-pit structure in an iron-silicon alloy which was made visible by diffusion of carbon atoms to the dislocations. Etch-pit techniques are useful because they can be used with bulk samples.

In certain systems it may be possible to distinguish between edge and screw dislocations and between positive and negative edge dislocations. The technique

¹ Several excellent reviews of experimental techniques have been published. See P. B. Hirsch, *Metall. Rev.*, vol. 4, no. 14, pp. 101–140, 1959; J. Nutting, *Seeing Dislocations*, in “The Structure of Metals,” Institution of Metallurgists, Interscience Publishers, Inc., New York, 1959; S. Amelinckx, *The Direct Observation of Dislocations*, *Solid State Phys. Suppl.*, 6, 1964.

² J. J. Gilman and W. G. Johnston, in “Dislocations and Mechanical Properties of Crystals,” John Wiley & Sons, Inc., New York, 1957.

³ J. D. Meakin and H. G. F. Wilsdorf, *Trans. Metall. Soc. AIME*, vol. 218, pp. 737–745, 1960.

⁴ A summary of etch-pit techniques in metals is given by L. C. Lowell, F. L. Vogel, and J. H.

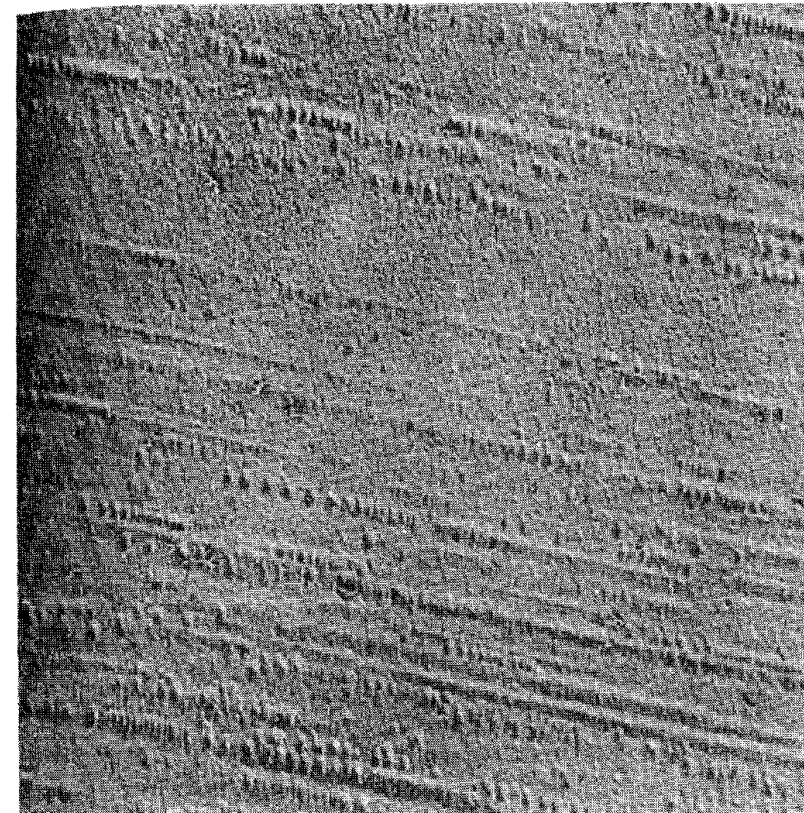


Figure 5-1 Etch pits on slip bands in alpha brass crystals ($5,000\times$). (From J. D. Meakin and H. G. F. Wilsdorf, *Trans. Metall. Soc. AIME*, vol. 218, p. 740, 1960.)

can also be used to study the movement of dislocations. However, care must be taken to ensure that pits are formed only at dislocation sites and that all dislocations intersecting the surface are revealed. Because the etch pits have a finite size and are difficult to resolve when they overlap, the etch-pit technique is limited generally to crystals with a low dislocation density of about 10^6 cm^{-2} (= 10^4 mm^{-2}).

A similar method of detecting dislocations is to form a visible precipitate along the dislocation lines. Usually a small amount of impurity is added to form the precipitate after suitable heat treatment. The procedure is called “decoration” of dislocations. This technique was first used by Hedges and Mitchell¹ to decorate dislocations in AgBr with photolytic silver. It has since been used with many other ionic crystals,² such as AgCl, NaCl, KCl, and CaF₂. With these optically transparent crystals this technique has the advantage that it shows the internal structure of the dislocation lines. Figure 5-2 shows a hexagonal network of dislocations in a NaCl crystal which was made visible by decoration. Although dislocation decoration has not been used extensively with metals, some work has

¹ J. M. Hedges and J. W. Mitchell, *Philos. Mag.*, vol. 44, p. 223, 1953.

² S. Amelinckx, in “Dislocations and Mechanical Properties of Crystals,” John Wiley & Sons, Inc.,



Introduction

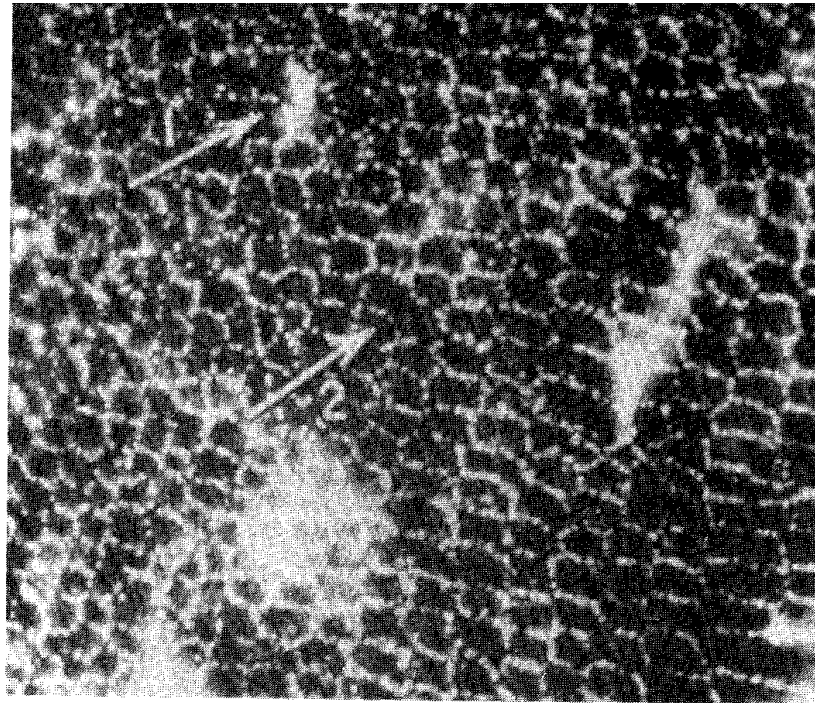


Figure 5-2 Hexagonal network of dislocations in NaCl detected by a decoration technique. (From S. Amelinckx, in: "Dislocations and Mechanical Properties of Crystals," John Wiley & Sons, Inc., New York, 1957. By permission of the publishers.)

been done along these lines with the Al-Cu precipitation-hardening system and with silicon crystals.

The most powerful method available today for the detection of dislocations in metals is transmission electron microscopy of thin foils.¹ Thin sheet, less than 1 mm thick, is thinned after deformation by electropolishing to a thickness of about 1,000 Å (= 100 nm). At this thickness the specimen is transparent to electrons in the electron microscope. In conventional transmission electron microscopy, individual dislocation lines can be observed because the intensity of the diffracted electron beam is altered by the strain field of the dislocation. The width of the diffraction image of a dislocation in a thin foil is about 100 Å (= 10 nm), so that this technique can be used at dislocation densities up to about 10^{11} cm^{-2} ($= 10^9 \text{ mm}^{-2}$). By means of this technique it has been possible to observe dislocation networks (Fig. 5-3), stacking faults, dislocation pile-up at grain boundaries (Fig. 6-1), Lomer-Cottrell barriers, and many other structural features of dislocation theory. Dislocation movement has been observed by generating thermal stresses

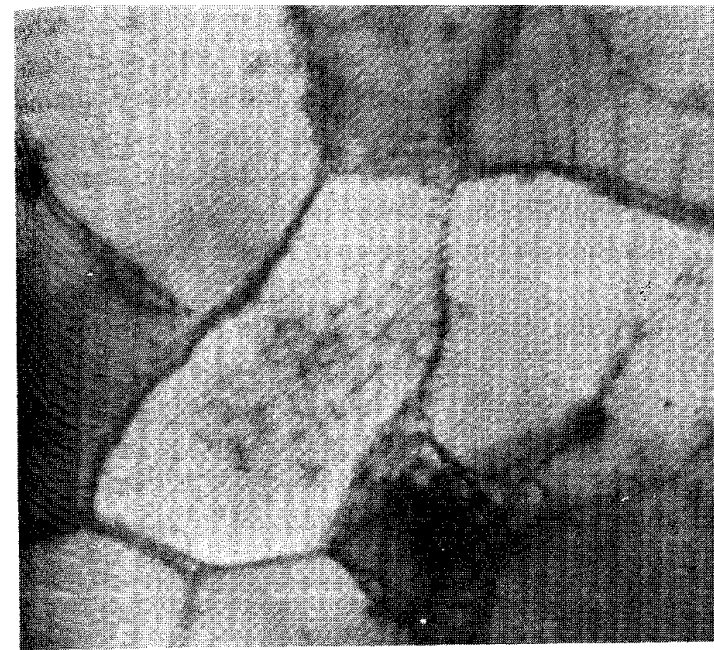


Figure 5-3 Dislocation network in cold-worked aluminum ($32,500 \times$). (From P. B. Hirsch, R. W. Horne, and M. J. Whelan, *Philos. Mag.*, ser. 8, vol. 1, p. 677, 1956.)

in the thin film with the electron beam or by using special straining fixtures in the electron microscope.¹

Transmission electron microscopy is the most powerful and universally applicable technique available for studying dislocations in solids. By application of the kinematic² and dynamic³ theories of electron diffraction, it is possible to make detailed analysis of the images to determine the number of dislocations, their Burgers vectors, and the slip planes on which they lie. However, this technique is not without disadvantages. Since only a miniscule volume of material is examined with thin films, great care must be exerted to obtain a representative sample. It is possible to alter the defect structure during sectioning and polishing to a thin film, and dislocation structures may relax in a very thin foil. The greatest defect of transmission electron microscopy is that it is not very effective in detecting long-range stresses, nor does it give very much information about slip-line lengths or surface step heights.

The dislocation structure of a crystal can be detected by x-ray microscopy. The most common techniques are the Berg-Barrett reflection method⁴ and the

Introduction

Lang topography method.¹ Unfortunately, the limiting resolution of these techniques is about 10^3 dislocations per square millimeter. Important features of plastically deformed metal such as the mean size of coherently diffracting domains (crystallite size), the microstrains within these domains, and the probability of lattice faulting can be determined by detailed analysis of the breadth and shape of x-ray diffraction peaks.² X-ray peak profile studies are indirect and statistical, and depend on models of the dislocation structure to relate their results to dislocation behavior.

The ultimate technique for observing defect structure is the field-ion microscope.³ Since its resolution is 2 to 3 Å (= 0.2 to 0.3 nm), individual atoms may be distinguished. Thus, it is the only experimental technique for directly observing vacancies. At its present state of development, field-ion microscopy is limited to metals with a strong binding force, such as W, Mo, or Pt. Since the specimen must be a fine wire bent into a sharp tip, the method is limited in applicability and examines only a very small area of the surface.

5-3 BURGERS VECTOR AND THE DISLOCATION LOOP

The Burgers vector \mathbf{b} is the vector which defines the magnitude and direction of slip. Therefore, it is the most characteristic feature of a dislocation. It has already been shown that for a *pure* edge dislocation the Burgers vector is perpendicular to the dislocation line, while for a *pure* screw dislocation the Burgers vector is parallel to the dislocation line. The macroscopic slip produced by the motion of an edge dislocation is shown in Fig. 5-4a and by a screw dislocation in Fig. 5-4b. Both the shear stress and final deformation are identical for both situations, but for an edge dislocation the dislocation line moves parallel to the slip direction while the screw dislocation moves at right angles to it. The geometric properties of dislocations are summarized in Table 5-1.

Actually, dislocations in real crystals are rarely straight lines and rarely lie in a single plane. In general, a dislocation will be partly edge and partly screw in character. As shown by Figs. 5-2 and 5-3, dislocations will ordinarily take the form of curves or loops, which in three dimensions form an interlocking dislocation network. In considering a dislocation loop in a slip plane any small segment of the dislocation line can be resolved into edge and screw components. For example, in Fig. 5-5, the dislocation loop is pure screw at point A and pure edge at point B, while along most of its length it has mixed edge and screw components. Note, however, that the Burgers vector is the same along the entire dislocation loop. If this were not so, part of the crystal above the slipped region would have to slip by a different amount relative to another part of the crystal

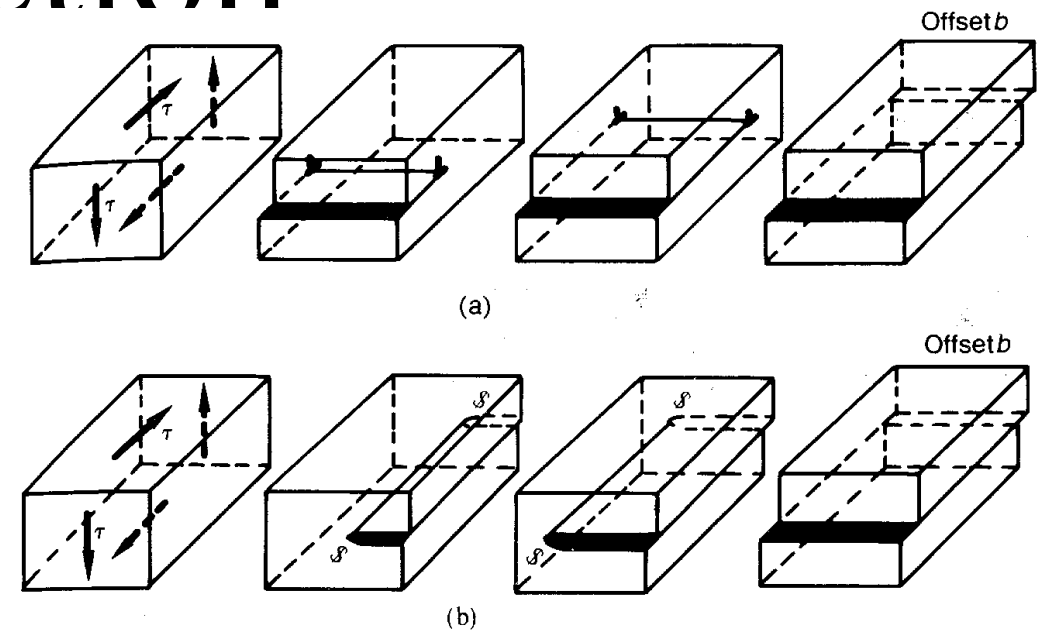


Figure 5-4 (a) Macroscopic deformation of a cube produced by glide of an edge dislocation. (b) Macroscopic deformation of a cube produced by glide of a screw dislocation. Note that the end result is identical for both situations.

Table 5-1 Geometric properties of dislocations

Dislocation property	Type of dislocation	
	Edge	Screw
Relationship between dislocation line and \mathbf{b}	perpendicular	parallel
Slip direction	parallel to \mathbf{b}	parallel to \mathbf{b}
Direction of dislocation line movement relative to \mathbf{b} (slip direction)	parallel	perpendicular
Process by which dislocation may leave slip plane	climb	cross-slip

and this would mean that another dislocation line would run across the slipped region.

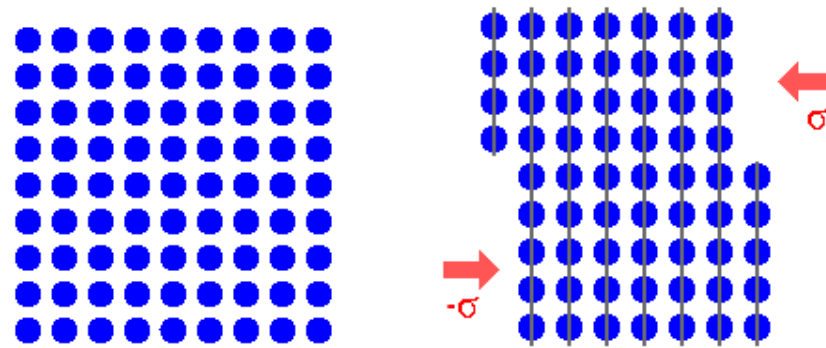
A convenient way of defining the Burgers vector of a dislocation is with a *Burgers circuit*. Consider the positive edge dislocation shown in Fig. 5-6a. If we start at a lattice point and imagine a clockwise path traced from atom to atom an equal distance in each direction, we find that at the finish of the path the circuit does not close. The closure failure from finish to start is the Burgers vector \mathbf{b} of the dislocation. (If we had made the Burgers circuit around the dislocation in the anticlockwise direction, the direction of the Burgers vector would have been in the opposite sense.) Moreover, if we traverse a Burgers circuit about the screw dislocation shown in Fig. 5-6b, we would find the closure error pointing out of the front face of the crystal. This is a right-handed screw dislocation since in

Introduction

Why metals could be plastically deformed?

Why the plastic deformation properties could be changed to a very large degree by forging without changing the chemical composition?

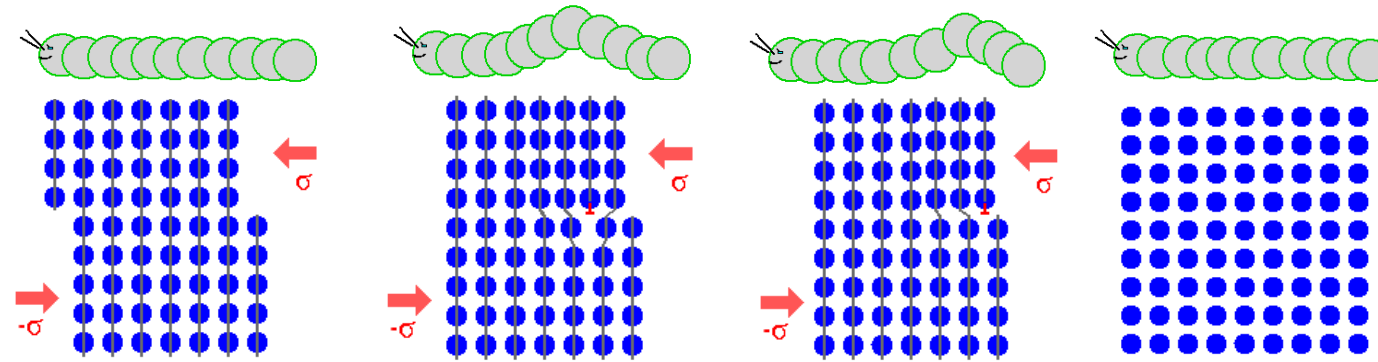
Why plastic deformation occurs at stresses that are much smaller than the theoretical strength of perfect crystals?



Plastic deformation – the force to break all bonds in the slip plane is much higher than the force needed to cause the deformation. Why?

These questions can be answered based on the idea proposed in 1934 by Taylor, Orowan and Polanyi: **Plastic deformation is due to the motion of a large number of dislocations.**

Dislocation allow deformation at much lower stress than in a perfect crystal

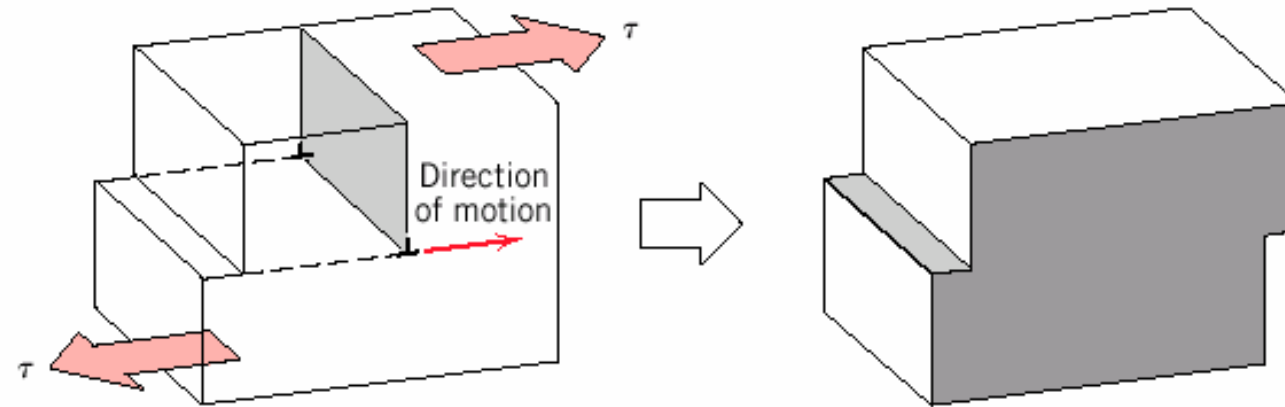


If the top half of the crystal is slipping one plane at a time then only a small fraction of the bonds are broken at any given time and this would require a much smaller force.

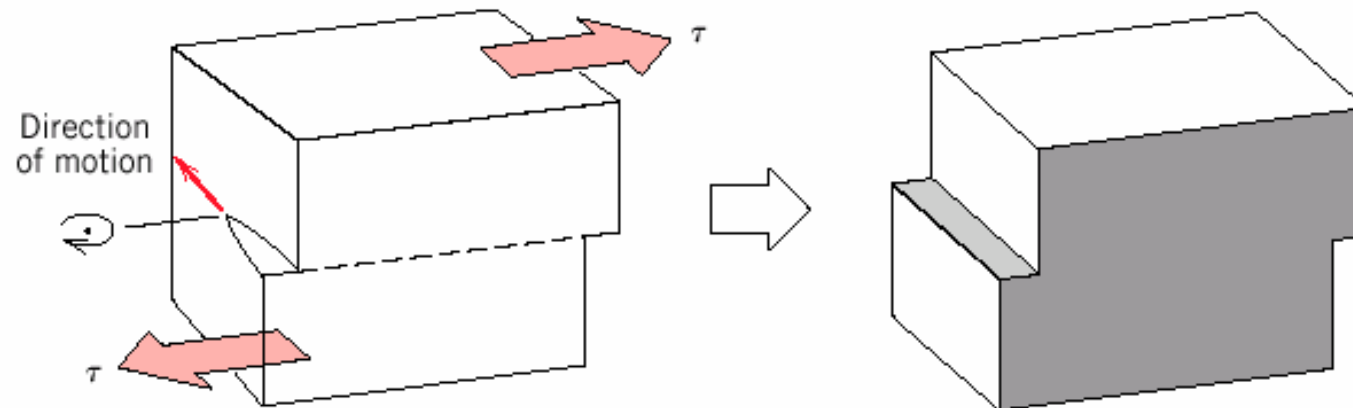
The propagation of one dislocation across the plane causes the top half of the crystal to move (**to slip**) with respect to the bottom half but we do not have to break all the bonds across the middle plane simultaneously (which would require a very large force).

The slip plane – the crystallographic plane of dislocation motion.

Direction of dislocation motion



Edge dislocation line moves parallel to applied stress



Screw dislocation line moves perpendicular to applied stress

For mixed dislocations, direction of motion is in between parallel and perpendicular to the applied shear stress

Dislocations in the FCC lattice

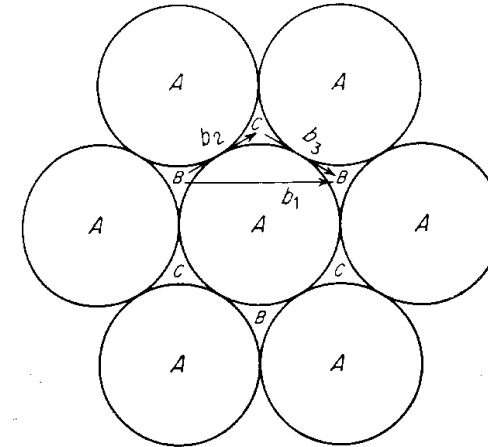


Figure 5-8 Slip in a close-packed (111) plane in an fcc lattice. (After A. H. Cottrell, "Dislocations and Plastic Flow in Crystals," p. 73, Oxford University Press, New York, 1953. By permission of the publishers.)

packing on a close-packed (111) plane. It has already been shown (Fig. 4-4) that the {111} planes are stacked on a sequence $ABCABC\dots$. The vector $b = (a_0/2)[10\bar{1}]$ defines one of the observed slip directions. The same shear displacement as produced by b_1 can be accomplished by the two-step path $b_2 + b_3$. The latter displacement is more energetically favorable but it causes the perfect dislocation to decompose into two partial dislocations.

$$\mathbf{b}_1 \rightarrow \mathbf{b}_2 + \mathbf{b}_3$$

$$\frac{a_0}{2}[10\bar{1}] \rightarrow \frac{a_0}{6}[2\bar{1}\bar{1}] + \frac{a_0}{6}[11\bar{2}]$$

The above reaction is energetically favorable since there is a decrease in strain energy proportional to the change $a_0^2/2 \rightarrow a_0^2/3$.

Original dislocation	Product of reaction	
$ \mathbf{b}_1 = a_0[\frac{1}{4} + 0 + \frac{1}{4}]^{1/2}$	$ \mathbf{b}_2 = a_0[\frac{4}{36} + \frac{1}{36} + \frac{1}{36}]^{1/2}$	
$ \mathbf{b}_1 = \frac{\sqrt{2}}{2} a_0$	$ \mathbf{b}_2 = \frac{a_0}{\sqrt{6}}$	$ \mathbf{b}_3 = \frac{a_0}{\sqrt{6}}$
$b_1^2 = \frac{a_0^2}{2}$	$> b_2^2 = \frac{a_0^2}{6}$	$b_3^2 = \frac{a_0^2}{6}$
b_1^2	$> b_2^2 + b_3^2$	

5-4 DISLOCATIONS IN THE FACE-CENTERED CUBIC LATTICE

Slip occurs in the fcc lattice on the {111} plane in the $\langle 110 \rangle$ direction. The shortest lattice vector is $(a_0/2)[110]$, which connects an atom at a cube corner with a neighboring atom at the center of a cube face. The Burgers vector is therefore $(a_0/2)[110]$.

However, consideration of the atomic arrangement on the {111} slip plane shows that slip will not take place so simply. Figure 5-8 represents the atomic

Slip by this two-stage process creates a stacking fault $ABCAC|ABC$ in the stacking sequence. As Fig. 5-9 shows, the dislocation with Burgers vector \mathbf{b}_1 has been dissociated into two *partial dislocations* \mathbf{b}_2 and \mathbf{b}_3 . This dislocation reaction was suggested by Heidenreich and Shockley,¹ and therefore this dislocation arrangement is often known as *Shockley partials*, since the dislocations are imperfect ones which do not produce complete lattice translations. Figure 5-9 represents the situation looking down on (111) along $[11\bar{1}]$. AB represents the perfect dislocation line having the full slip vector \mathbf{b}_1 . This dissociates according to

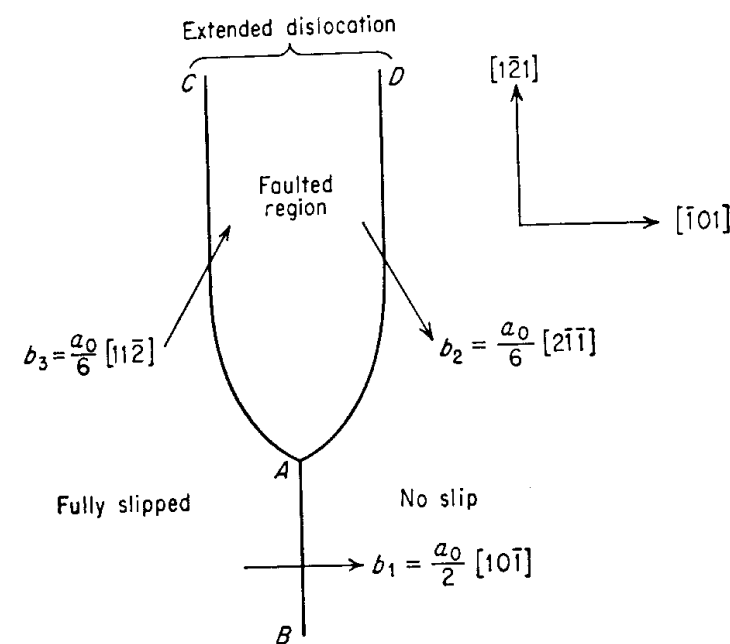


Figure 5-9 Dissociation of a dislocation into two partial dislocations.

the above reaction into partial dislocations with Burgers vectors \mathbf{b}_2 and \mathbf{b}_3 . The combination of the two partials AC and AD is known as an *extended dislocation*. The region between them is a stacking fault representing a part of the crystal which has undergone slip intermediate between full slip and no slip. Because \mathbf{b}_2 and \mathbf{b}_3 are at a 60° angle, there will be a repulsive force between them (Sec. 5-9). However, the surface tension of the stacking fault tends to pull them together. The partial dislocations will settle at an equilibrium separation determined primarily by the stacking-fault energy. As was discussed in Sec. 4-11, the stacking-fault energy can vary considerably for different fcc metals and alloys and this in turn can have an important influence on their deformation behavior.

Dissociation of unit dislocations is independent of the character (edge, screw, or mixed) of the dislocation. However, unlike the unextended screw dislocation, the extended screw dislocation defines a specific slip plane, the $\{111\}$ plane of the fault, and it will be constrained to move in this plane. The partial dislocations move as a unit maintaining the equilibrium width of the faulted region. Because of this restriction to a specific slip plane, an extended screw dislocation cannot cross slip unless the partial dislocations recombine into a perfect dislocation. Constrictions in the stacking fault ribbon which permit cross slip are possible (Fig. 4-28), but this requires energy. The greater the width of the stacking fault (or the lower the stacking-fault energy) the more difficult it is to produce constrictions in the stacking faults. This explains why cross slip is quite prevalent in aluminum, which has a very narrow stacking-fault ribbon, while it is not observed usually in copper, which has a wide stacking-fault ribbon.

Extended dislocations are readily detected by transmission electron microscopy. Figure 5-10 shows the characteristic fringe pattern of the stacking fault between the extended dislocations.

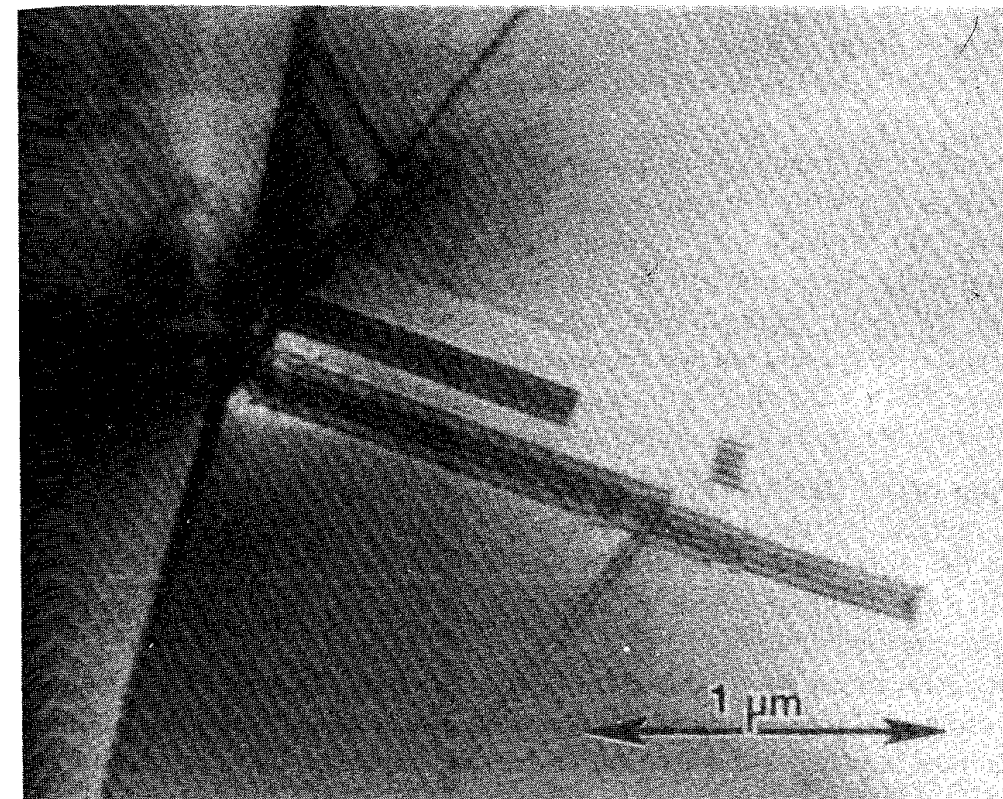


Figure 5-10 Group of stacking faults in 302 stainless steel stopped at boundary on left-hand side. (Courtesy of Prof. H. G. F. Wilsdorf, University of Virginia.)

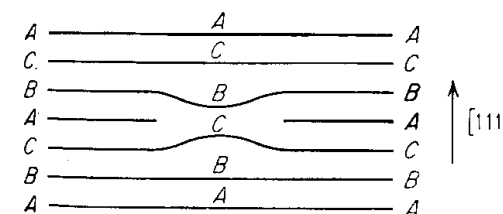


Figure 5-11 A Frank partial dislocation or sessile dislocation. (After A. H. Cottrell, "Dislocations and Plastic Flow in Crystals," p. 75, Oxford University Press, New York, 1953. By permission of the publishers.)

Frank¹ pointed out that another type of partial dislocation can exist in the fcc lattice. Figure 5-11 illustrates a set of (111) planes viewed from the edge. The center part of the middle A plane is missing. An edge dislocation is formed in this region with a Burgers vector $(a_0/3)[111]$. This is called a *Frank partial dislocation*. Its Burgers vector is perpendicular to the central stacking fault. Since glide must be restricted to the plane of the stacking fault and the Burgers vector is normal to this plane, the Frank partial dislocation cannot move by glide. For this reason it is called a *sessile dislocation*. A sessile dislocation can move only by the diffusion of atoms or vacancies to or from the fault, i.e., by the process of climb. Because climb is not a likely process at ordinary temperatures, sessile dislocations provide obstacles to the movement of other dislocations. Dislocations which glide freely

¹ F. C. Frank, *Proc. Phys. Soc. London*, vol. 62A, p. 202, 1949.

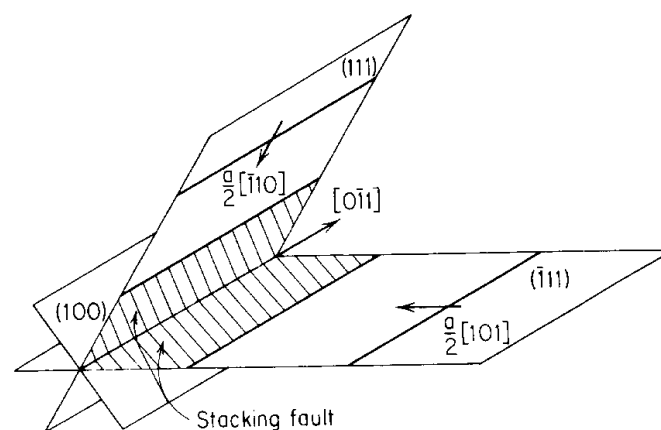


Figure 5-12 Lomer-Cottrell barrier.

over the slip plane, such as perfect dislocations or Shockley partials, are called *glissile*. A method by which a missing row of atoms can be created in the (111) plane is by the condensation of a disk of vacancies on that plane. Evidence for the collapse of disks of vacancies in aluminum has been obtained by transmission electron microscopy.¹

Sessile dislocations are produced in the fcc lattice by the glide of dislocations on intersecting {111} planes during duplex slip. The sessile dislocation produced by the reaction is called a *Lomer-Cottrell barrier*. Consider two perfect dislocations $a_0/2[\bar{1}10]$ and $a_0/2[101]$ lying in different {111} planes and both parallel to the line of intersection of the {111} planes (Fig. 5-12). These dislocations attract each other and move toward their line of intersection. Lomer² suggested that they react according to

$$\frac{a_0}{2}[101] + \frac{a_0}{2}[\bar{1}10] \rightarrow \frac{a_0}{2}[011]$$

to produce a new dislocation of reduced energy. This new dislocation lies parallel to the line of intersection of the initial slip planes in the (100) plane bisecting the slip planes. Its Burgers vector lying in the (100) plane is normal to the line of intersection so it is a pure edge dislocation. Since (100) is not a close-packed slip plane in the fcc lattice, this dislocation will not glide freely. However, it is not a true sessile dislocation in the sense of the Frank partial because it is not an imperfect dislocation.

Cottrell³ showed that the product of Lomer's reaction could be made strictly immobile if it is considered that dislocations on the {111} planes of an fcc metal are normally dissociated into partials. The leading partial dislocations on each slip plane will interact with each other in a reaction of the type

$$\frac{a_0}{6}[\bar{1}2\bar{1}] + \frac{a_0}{6}[1\bar{1}2] \rightarrow \frac{a_0}{6}[011]$$

¹ P. B. Hirsch, J. Silcox, R. E. Smallman, and K. H. Westmacott, *Philos. Mag.*, vol. 3, p. 897, 1958.

² W. M. Lomer, *Philos. Mag.*, vol. 42, p. 1327, 1951.

³ A. H. Cottrell, *Philos. Mag.*, vol. 43, p. 645, 1952.

Like before, the new dislocation $a_0/6[011]$ lies parallel to the line of intersection of the slip plane and has a pure edge character in the (100) plane. The dislocation is sessile because its Burgers vector does not lie in either of the planes of its stacking faults.

Lomer-Cottrell barriers can be overcome at high stresses and/or temperatures. A mathematical analysis of the stress required to break down a barrier either by slip on the (100) plane or by reaction back into the dislocations from which the barrier formed has been given by Stroh.¹ However, it has been shown² that for the important case of screw dislocations piled up at Lomer-Cottrell barriers, the screw dislocations can escape the pile-up by cross slip before the stress is high enough to collapse the barrier. While the formation of Lomer-Cottrell barriers is an important mechanism in the strain hardening of fcc metals, they do not constitute the chief contribution to strain hardening.

Because of the multiplicity of slip systems in the fcc lattice, a large number of dislocation reactions of the types discussed above are possible. These have been worked out in detail by Hirth.³ Also, the Thompson tetrahedron⁴ is a useful geometrical method for visualizing the geometry of these reactions.

5-5 DISLOCATIONS IN THE HEXAGONAL CLOSE-PACKED LATTICE

The basal plane of the hcp lattice is a close-packed plane with the stacking sequence *ABABAB*... Slip occurs on the basal plane (0001) in the $\langle 11\bar{2}0 \rangle$ direction (Fig. 4-3). The smallest unit vector for the hcp structure has a length a_0 and lies in the close-packed $\langle 11\bar{2}0 \rangle$ direction. Therefore, the Burgers vector is $(a_0/3)[11\bar{2}0]$. Dislocations in the basal plane can reduce their energy by dissociating into Shockley partials according to the reaction

$$\frac{a_0}{3}[11\bar{2}0] \rightarrow \frac{a_0}{3}[10\bar{1}0] + \frac{a_0}{3}[01\bar{1}0]$$

The stacking fault produced by this reaction lies in the basal plane, and the extended dislocation which forms it is confined to glide in this plane.

5-6 DISLOCATIONS IN THE BODY-CENTERED CUBIC LATTICE

Slip occurs in the $\langle 111 \rangle$ direction in the bcc lattice. The shortest lattice vector extends from an atom corner to the atom at the center of the unit cube. Therefore, the Burgers vector is $(a_0/2)[111]$. It will be recalled that slip lines in iron have been found to occur on {110}, {112}, and {123}, although in other bcc

¹ A. N. Stroh, *Philos. Mag.*, vol. 1, sec. 8, p. 489, 1956.

² A. Seeger, J. Diehl, S. Mader, and R. Rebstock, *Philos. Mag.*, vol. 2, p. 323, 1957.

³ J. P. Hirth, *J. Appl. Phys.*, vol. 32, pp. 700-706, 1961.

⁴ N. Thompson, *Proc. Phys. Soc. London Ser. B*, vol. B66, p. 481, 1953.